The Open Medicinal Chemistry Journal
DOI: 10.2174/0118741045420705251028094550, 2026, 20, e18741045420705
ISSN: 1874-1045
1

RESEARCH ARTICLE OPEN ACCESS

Therapeutic Potential of Ertugliflozin in Renal Ischemia/Reperfusion Injury by Modulating Nrf2 and Necroptosis Pathways: A Preclinical Study in Rats

Ali F. Jaber[1,*] and Ali M. Janabi[2]

[1]*Karbala Health Directorate, Imam Hussain Medical City, Karbala, Iraq*
[2]*Department of Pharmacology and Toxicology, Faculty of Pharmacy, University of Kufa, Najaf, Iraq*

Abstract:

Introduction: Renal ischemia/reperfusion injury is a sequence of complicated events that involve a reduction in blood supply followed by a recovery of perfusion and oxygenation to the kidneys. Ertugliflozin is a selective inhibitor of SGLT2. To our best knowledge, there is limited published data about the nephroprotective effects of ertugliflozin *via* the Nrf2 and RIPK1/MLKL molecular pathways. The aim of this study is to investigate the nephroprotective effects of ertugliflozin through Nrf2 and RIPK1/MLKL molecular pathways.

Materials and Methods: 24 Sprague Dawley rats were assigned to four groups: Sham, I/R, I/R + Veh, and I/R + EGZ. The sham group underwent laparotomy without induction of the I/R model. The other three groups were subjected to 30 minutes of bilateral renal ischemia and 24 hours of reperfusion. The I/R + Veh and I/R + EGZ groups received DMSO and 20 mg/kg ertugliflozin intraperitoneally one hour before ischemia induction, respectively.

Results: KIM-1, TNF-α, IL-1β, NF-κB, and caspase-3 levels were quantified using ELISA. Nrf2 and MLKL were assessed through IHC, while RIPK1 expression was determined *via* RT-qPCR, in addition to histopathological examination. In I/R and I/R + Veh groups, KIM-1, TNF-α, IL-1β, NF-κB, caspase-3, RIPK1, MLKL, and histopathological findings were remarkably elevated. On the contrary, the administration of ertugliflozin substantially reduced renal damage, inflammation, cell death, and histological features. Nuclear translocation of Nrf2 was greatly increased in the ertugliflozin-treated group, and molecular docking revealed that ertugliflozin was bound to Keap1.

Discussion: The administration of ertugliflozin notably increased the Nrf2 expression. These findings, along with the reduction in renal damage, Necroptosis, and apoptosis, indicate the nephroprotective effect of ertugliflozin.

Conclusion: Ertugliflozin showed marked nephroprotective effects evidenced by reduced oxidation, inflammation, Necroptosis, apoptosis, and necrosis through translocation of Nrf2 and inhibition of RIPK1/MLKL pathways.

Keywords: Ertugliflozin, Renal ischemia/reperfusion injury, Nrf2, RIPK1, MLKL, Necroptosis.

*Address correspondence to this author at the Karbala Health Directorate, Imam Hussain Medical City, Karbala, Iraq; E-mail: ph.alifaisal@gmail.com

Cite as: Jaber A, Janabi A. Therapeutic Potential of Ertugliflozin in Renal Ischemia/Reperfusion Injury by Modulating Nrf2 and Necroptosis Pathways: A Preclinical Study in Rats. Open Med Chem J, 2026; 20: e18741045420705.
http://dx.doi.org/10.2174/0118741045420705251028094550

Received: July 07, 2025
Revised: September 24, 2025
Accepted: October 21, 2025
Published: January 08, 2026

1. INTRODUCTION

Renal Ischemia/Reperfusion Injury (IRI) is a sequence of complicated events involving a reduction in blood supply followed by recovery of perfusion and oxygenation to the kidneys [1]. It includes both local and systemic effects and primarily involves two steps: first, ischemia, where the Adenosine Triphosphate (ATP) loss occurs, and second, reperfusion, during which the oxidative stress, inflammation, and cell death occur [2]. IRI frequently occurs during cardiovascular procedures, cardiogenic shock, or organ transplantation [3]. Immunologically, innate immunity is the key component of the early response to IRI; it includes various types of cells, like neutrophils and monocytes/macrophages. On the other hand, adaptive immunity comprises antigen-presenting, dendritic cell maturation, T cell proliferation and activation, and lymphocyte interactions [4]. Physiologically, the generation and scavenging of Reactive Oxygen Species (ROS) are dynamically equilibrated. Once this equilibrium is disturbed by the overproduction of ROS and the reduction of antioxidant defenses, oxidative stress happens, promoting inflammation and cellular damage [5, 6]. Nuclear factor erythroid 2-related factor 2 (Nrf2) is the major transcription factor regulator of oxidative stress, participating in cytoprotection, redox homeostasis, drug metabolism, iron and amino acid metabolism, cellular proliferation, and other physiological functions [7]. Physiologically, two molecules of kelch-like ECH-associated protein 1 (Keap1) homodimerize with two Nrf2 motifs and then with Cullin-3/RING-box protein, ubiquitinating the lysine residue of Nrf2. Consequently, Nrf2 is removed and degraded while Keap1 is reutilized again. This process will sequester the Nrf2 and prevent its nuclear translocation [8]. Conversely, during oxidative stress, the cysteine residue of Keap1 is oxidized, triggering a conformational change and the separation of Keap1. As a result, the Nrf2 is released, translocates to the nucleus, and heterodimerizes with the small Musculoaponeurotic fibrosarcoma (sMaf). This complex interacts with antioxidant response elements, activating downstream cytoprotective genes [9]. Necroptosis was first described in 2005 as a cellular programmed pathway of necrosis. It is pro-inflammatory, non-caspase-dependent, and shares features of both apoptosis and necrosis. On the one hand, it is similar to apoptosis in that it is strictly regulated and initiated by certain signals, while on the other hand, it is morphologically resembling necrosis, where the cells are ruptured, resulting in the leaking of damage-associated molecular patterns with the subsequent inflammation [10, 11]. Stressful conditions like IRI, drugs, calcium overload, and heat and osmotic stress can activate necroptosis through several ligand/receptor signaling pathways, among which the Tumor Necrosis Factor-alpha (TNF-α)//TNF Receptor (TNFR) 1 interaction is the most studied one [12]. The consequences of TNF-α/TNFR1 interaction are cellular survival, apoptosis, or necroptosis [13]. Ertugliflozin is a selective inhibitor of Sodium-Glucose Cotransporter-2 (SGLT2). It is the newest member of the SGLT2 inhibitor family and, together with diet and physical activity, lowers blood glucose in diabetic patients [14, 15]. In healthy euglycemic individuals, the glomerulus filters about 180 grams of glucose each day. Most of the glucose is reclaimed from the proximal tubule by SGLT2, accounting for more than 90% of glucose reabsorption [16]. Ertugliflozin selectively blocks SGLT2, limiting glucose reabsorption from the kidney, increasing glucose excretion in urine, and lowering blood sugar and glycated hemoglobin A1c [17].

Additionally, it reduces body weight by reducing calories from glycosuria, lowers blood pressure due to its natriuretic and diuretic effects, and significantly benefits the kidney and cardiovascular system [18]. There are limited published data on the nephroprotective impacts of ertugliflozin through Nrf2 and Receptor-Interacting Serine/Threonine-Protein Kinase 1 (RIPK1)/ Mixed Lineage Kinase Domain-like Pseudokinase (MLKL) molecular pathways in renal IRI. This study aims to investigate the nephroprotective effects of ertugliflozin through Nrf2 and RIPK1/MLKL molecular pathways and by assessing inflammatory and cell death markers.

2. MATERIALS AND METHODS

2.1. Chemicals and Assay Kits

Ertugliflozin (CAS No. 1210344-57-2, MW: 436.88, purity: 99%) was purchased from Macklin Biochemical Technology, China. Dimethyl Sulfoxide (DMSO) (CAS No. 67-68-5, MW: 78.13) was purchased from CDH, India. Ketamine (10%) and xylazine (2%) were purchased from Alfasan, Netherlands. Rat ELISA kits for KIM-1 (Cat. No. SL0433Ra), TNF-α (Cat. No. SL0722Ra), Interleukin-1 beta (IL-1β) (Cat. No. SL0402Ra), Nuclear Factor kappa-light-chain-enhancer of activated B cells (NF-kB) (Cat. No. SL0537Ra), and caspase-3 (Cat. No. SL0152Ra) were purchased from Sunlong, China. Nrf2 (Cat. No. E-AB-93081) and MLKL (Cat. No. E-AB-67102) polyclonal antibody IHC kits were purchased from ELABSCINE, China. GoTaq® 1-Step RT-qPCR system (Cat. No. A6020), AddScript cDNA synthesis kit (Cat. No. 22701), RIPK1 and GAPDH primers, and Easy-spin™ (DNA-free) total RNA extraction kit (Cat. No. 17221) were purchased from Promega/USA, Addbio/Korea, Macrogen/Korea, and Intron/Korea, respectively.

2.2. Animals

The resource equation method [19] was utilized for sample size calculation, as estimating the effect size was challenging. Since the study included four groups, the total number of animals ranged from 16 to 24. Therefore, 24 animals were used. Twenty-four male Sprague-Dawley rats, about eight weeks of age, and 200-250 grams in weight were used in the current study. They were obtained from the Faculty of Sciences at the University of Kufa, Najaf, Iraq. Rats were kept in separate cages, with water and diet ad libitum, under-regulated environments of a temperature of 25 ± 2°C and a 12-hour light and dark cycle. After the surgery, each rat was kept in a cage until the sample collection. After a two-week adaptation period, rats were used in the study. The inclusion criteria were healthy male rats of the age and weight mentioned earlier.

2.3. Animal Ethical Approval

The policy of the University of Kufa for scientific purposes was followed in the care and usage of animals. Pain, distress, and discomfort were avoided or minimized by anesthetizing rats with a mixture of ketamine and xylazine based on their body weight. Upon completion of the procedure, a high dose of anesthesia was used to euthanize the rats. The Central Committee of Bioethics at the University of Kufa, Iraq, approved all the procedures and experimental design (Approval No. 20554) on August 29, 2024. This research complies with internationally accepted standards for animal studies and adheres to the 3Rs principle. The ARRIVE criteria were utilized to promote ethical research practices.

2.4. Experimental Design

Rats were assigned randomly into four groups (six rats each):

[A] Sham group: rats were anesthetized and underwent laparotomy without Ischemia/Reperfusion (I/R)

[B] I/R group: rats were anesthetized and subjected to 30 minutes of bilateral renal ischemia, then 24 hours of reperfusion.

[C] I/R+Vehicle group (I/R+Veh): This group is similar to the I/R group, but the ertugliflozin (10% DMSO) solution was administered intraperitoneally (I.P.) 1 hour before bilateral renal ischemia.

[D] I/R + ertugliflozin (I/R + EGZ) group: It is similar to the I/R group, but 20 mg/kg of ertugliflozin was administered [20, 21] to the animals by the I.P. route one hour before bilateral renal ischemia.

2.5. Model of Renal Ischemia/Reperfusion Injury

Renal I/R was performed based on several scientific studies [22-25]. Under aseptic conditions, rats were anesthetized with a combination of I.P. 100 mg of ketamine and 10 mg of xylazine per kg of the rat's weight [26, 27]. The extent of anesthesia is examined by the tail pinch and pedal reflex. Afterward, rats were placed supine by fixing their limbs with surgical plaster. A midline laparotomy was made, the intestine was retracted, and the renal pedicle was exposed. Bilateral ischemia was induced by clamping the renal blood vessels with non-traumatic microvascular clamps for 30 minutes; the ischemic phase was examined visually by changing the kidneys' color. To keep rats well hydrated, 1ml of 0.9% normal saline was injected into the abdomen, then the abdomen was covered with wet, warm gauze. After 30 minutes of ischemia, the clamps were removed, and the reperfusion phase began, which was visually assessed by changes in kidney color. The abdominal incision was sutured in two layers with zero nylon surgical sutures, disinfected with 10% povidone-iodine, and covered with surgical plaster. The reperfusion phase lasted 24 hours; afterward, rats were anesthetized again for tissue and blood collection. Lastly, rat euthanasia was done with a high dose of anesthesia [28].

2.6. Tissue Collection

At the end of the 24-hour reperfusion phase, both kidneys were harvested. The left kidney was divided into two halves, put in an Eppendorf tube, and snap-frozen in liquid nitrogen. One-half was used to measure the gene expression of RIPK1 by RT-qPCR, while the other half was used for measuring KIM-1, TNF-α, IL-1β, NF-κB, and caspase-3 levels using the ELISA technique. The right kidney was preserved in 10% formalin and stored until used for measuring Nrf2 and MLKL by the Immuno-histochemistry (IHC) technique and for Hematoxylin and Eosin (H&E) staining.

2.7. Tissue Preparation

For ELISA and RT-qPCR, tissue was prepared by thawing the kidney and cleaning it with Phosphate Buffer Saline (PBS). Then, the kidney was weighed and homogenized in 1:10 PBS containing 1% Triton X-100 with a cocktail of protease inhibitors. More homogenization was performed using a high-intensity ultrasonic liquid processor to obtain the supernatant, which was used to measure levels of KIM-1, TNF-α, IL-1β, NF-κB, and caspase-3 in tissue by ELISA, and RIPK1 by RT-qPCR.

2.8. Docking Study

The BTB domain of KEAP1 was obtained from the Protein Data Bank (PDB ID: 4CXI). The protein preparation, performed using MOE software 2015, involved removing aqueous solvent molecules to enhance the receptor/ligand interactions and adding protons to enhance protein preparation. The two-dimensional structure of ertugliflozin was designated by Chem-Bio Draw pro19.0. MOE was used to protonate the three-dimensional structure, assign partial charges, and minimize the energy. Ertugliflozin was docked, and the pose exhibiting a higher S-score with an appropriate RMSD value was chosen.

2.9. Renal Histopathology

The formalin-fixed kidney was processed through various tissue processing steps using an automated tissue processor. A microtome was used to obtain 5-um sections of paraffin blocks, which were mounted on slides for tissue staining. The slides were then de-paraffinized, rehydrated, washed, and stained with H&E. An independent histo-pathologist blinded to experimental groups examined the histopathological changes. The degree of tubular damage was scored from 0 to 4, where 0 indicates no damage, 1 signifies less than 25%, 2 represents 25-50%, 3 denotes 50-75%, and 4 exceeds 75% [29].

2.10. IHC Staining

The slides were de-waxed with xylene, rehydrated by immersing them in descending concentrations of ethanol, and rinsed with distilled water. The slides were incubated in the retrieval solution in a water bath, cooled to room temperature, and rinsed with the washing buffer solution to unmask the sample antigens. Peroxidase, a blocking agent, prevented non-specific binding. The post-protein block was applied for five minutes, and then washed again. The primary antibodies against Nrf2 and MLKL

were diluted to 1:100, applied to the slides, incubated, and washed with buffer solution. Consequently, the secondary antibody was added to the slides. The next steps include adding horseradish peroxidase, chromogen, and hematoxylin (the counterstain). As in H&E staining, levels of Nrf2 and MLKL were examined by an independent histopathologist blinded to study groups. The quick H-score was used to quantify the Nrf2 and MLKL, as described by Charafe-Jauffret *et al*. [30] and Parris *et al*. [31].

2.11. Gene Expression

Total RNA extraction was performed using the Easy-spin™ kit. Then, cDNA was synthesized using the AddScript cDNA Synthesis Kit. Primers were made according to the manufacturer's instructions. They were reconstituted with double-distilled water to a stock solution of 100 pM/µl, which was stored at -20°C. A 10 pM/µl concentration was produced as a working primer. Lastly, the gene expression assay was performed using the GoTaq® RT-qPCR System protocol. The 2^-ΔΔCT technique was employed to examine the gene expression data. For RIPK1, the 5'-3' sequence was GACCGAGTTCACAACCACCA (forward) and TGTTAGCGAAGACGGCTTGA (reverse), the product (bp) was 75, and the accession number was XM_017600528.3. For GAPDH, the 5'-3' sequence was ATGACTCTACCCA CGGCAAG (forward) and CTGGAAGATGGTGATGGGTT (reverse), the product (bp) was 89, and the accession number was NM_017008.

2.12. Statistical Analysis

The normality test was done using the Shapiro-Wilk test. For parametric data, the one-way Analysis of Variance (ANOVA) was applied to check the significant differences among study groups, and multiple comparisons were conducted using the Tukey post-hoc test. Nuclear Nrf2 and histopathological examination (nonparametric data) were assessed using the Kruskal–Wallis test, and pairwise comparisons were done by the Mann–Whitney U test. Data were presented as mean ± Standard Deviation (SD). GraphPad Prism v10.0 and IBM SPSS Statistics v26.0 were utilized to perform statistical analysis. Data visualization was generated *via* GraphPad Prism v10.0.

3. RESULTS

The descriptive statistics of the study parameters are presented in Table **1**.

3.1. Ertugliflozin Lowers the Damage Marker in the Renal IRI Model

To evaluate the effect of ertugliflozin on renal function, KIM-1 was measured in renal tissue. The model of I/R extremely increases the level of KIM-1 as seen in I/R ($p < 0.01$) and I/R + Veh ($p < 0.001$) groups, in contrast to the sham group. Conversely, ertugliflozin statistically lowered the KIM-1 level ($p < 0.05$); nevertheless, no substantial variation was observed between I/R and I/R + Veh groups ($p > 0.05$) (Fig. **1**).

3.2. Ertugliflozin Binds with Keap1

Molecular docking explained that ertugliflozin interacted with Keap1 through His129 and His154 (Fig. **2**).

3.3. Ertugliflozin Increases the Nuclear Localization of Nrf2

To investigate the effect of ertugliflozin on Nrf2, we measured cytoplasmic and nuclear Nrf2. Regarding cytoplasmic Nrf2, there was a non-statistical variation among all study groups ($p > 0.05$). However, nuclear Nrf2 was substantially elevated in the group of ertugliflozin relative to the sham, I/R, and I/R + Veh groups ($p < 0.0001$) (Table **2** and Fig. **2**).

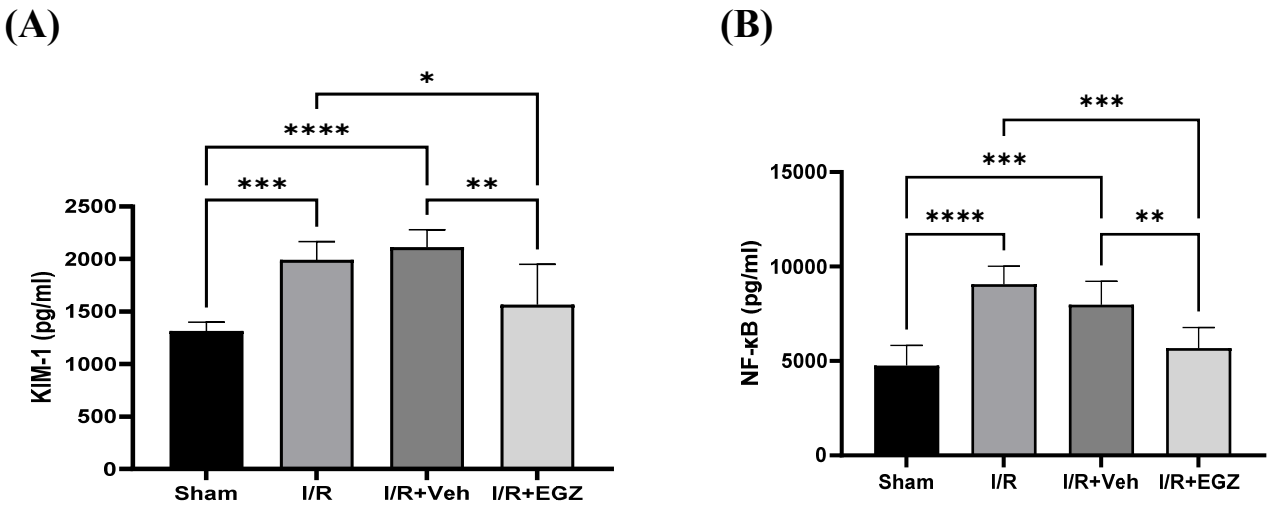

Fig. 1 contd.....

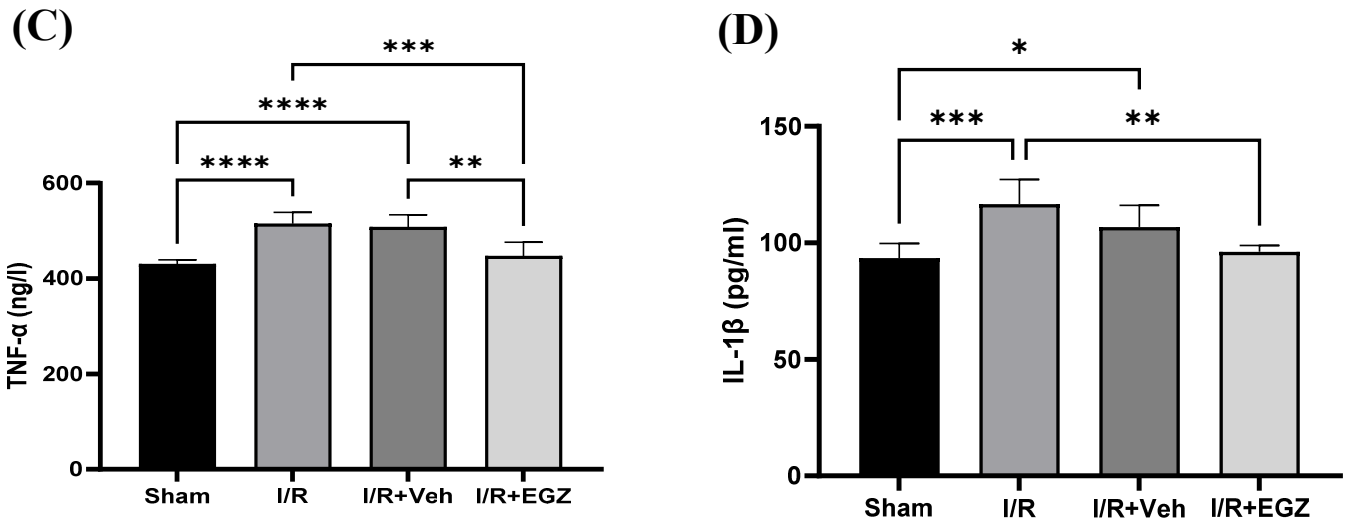

Fig. (1). Effect of ertugliflozin on renal damage, inflammatory, and oxidative stress markers in a rat model of I/R. **(A)** KIM-1. **(B)** NF-κB **(C)** TNF-α **(D)** IL-1β. The sham group underwent laparotomy without induction of the I/R model. The I/R, I/R+Veh, and I/R+EGZ groups were subjected to 30 minutes of bilateral renal ischemia and 24 hours of reperfusion. The I/R+Veh and I/R+EGZ groups received the solvent and 20 mg/kg of ertugliflozin intraperitoneally one hour before the ischemia induction, respectively. All markers were measured in renal tissue using the ELISA technique. Data expressed as Mean ± SD, *$p < 0.05$, **$p < 0.01$, ***$p < 0.001$.

Table 1. Descriptive statistics of the study parameters.

Biomarkers	Mean ± SD			
	Sham	I/R	I/R+Veh	I/R+EGZ
KIM-1 (pg/ml)	1311±85.90	1988±177.9	2110±169.1	1565±384.0
NF-κB (pg/ml)	4765±1049	9055±954.1	7972±1246	5679±1100
TNF-α (ng/l)	430.4±8.528	514.7±24.07	507.9±25.82	447.2±29.13
IL-1β (pg/ml)	93.43±6.373	116.7±10.48	106.8±9.363	96.25±2.750
Cytoplasmic Nrf2 (Quick H-score)	21.67±18.62	26.50±12.08	25.00±20.00	25.00±13.78
Nuclear Nrf2 (Quick H-score)	0.000±0.000	0.000±0.000	0.000±0.000	12.00±6.841
Caspase-3 (ng/ml)	4.363±0.6860	5.913±0.4938	6.384±0.4870	4.660±0.6091
RIPK1 (2^-Δ Δ CT)	1.000±0.000	4.147±0.3138	3.369±0.9125	0.4867±0.2569
MLKL (Quick H-score)	35.50±17.41	177.2±45.70	160.7±37.45	55.83±44.77
Histopathological examination (Damage score)	0.000±0.000	3.833±0.4082	4.000±0.000	2.833±0.4082

Note: I/R ischemia/reperfusion, Vehicle (Veh), EGZ ertugliflozin, KIM-1 Kidney Injury Molecule-1, NF-κB Nuclear Factor Kappa-light-chain-enhancer of activated B cells, TNF-α Tumor Necrosis Factor-alpha, IL-1β Interleukin-1 beta, Nrf2 Nuclear Factor Erythroid 2-related factor 2, RIPK1 Receptor-Interacting Serine/Threonine-Protein Kinase 1, MLKL Mixed Lineage Kinase Domain-like Protein.

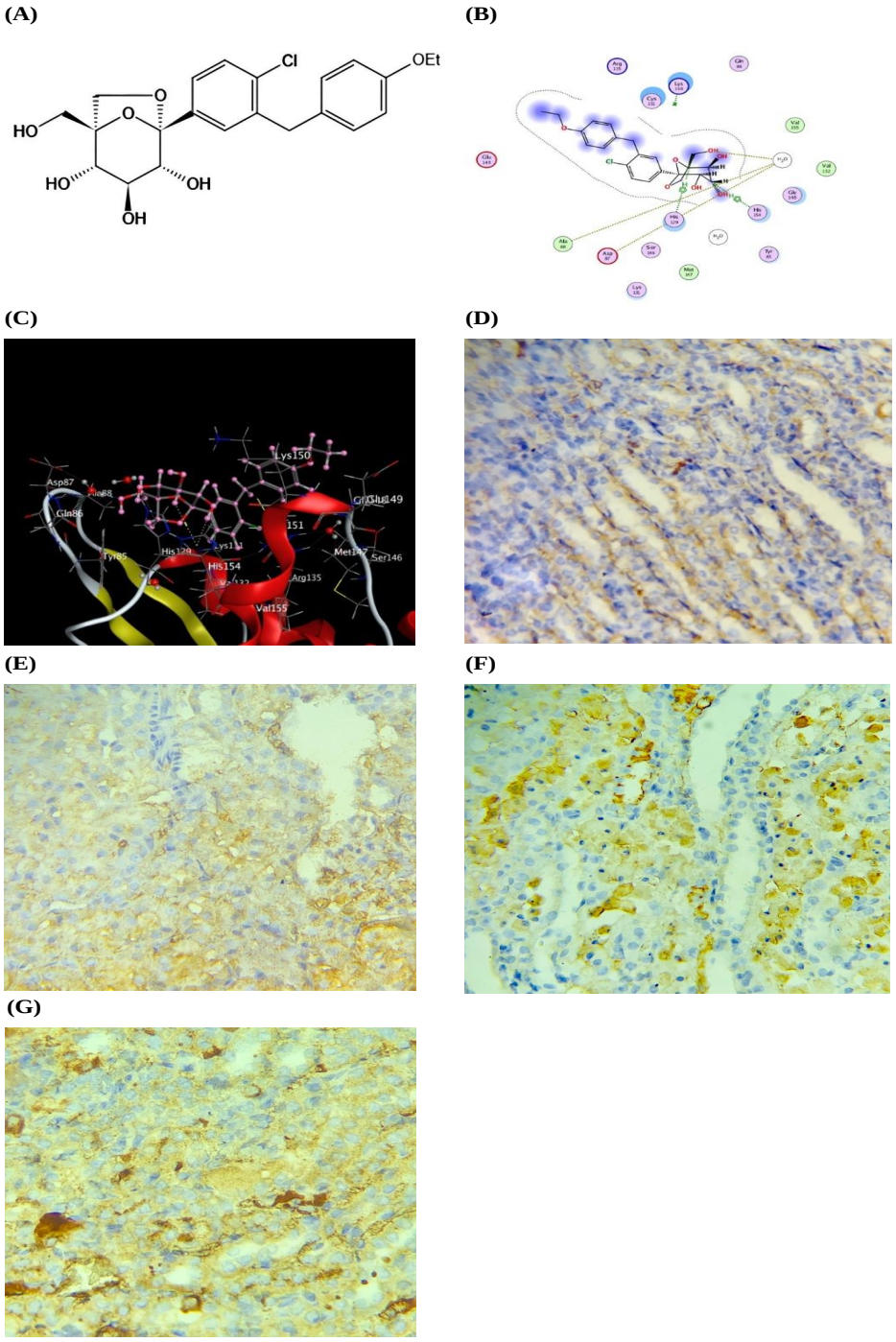

Fig. (2). Effect of ertugliflozin on cytoplasmic and nuclear Nrf2 in a rat model of I/R. **(A)** Chemical structure of ertugliflozin. **(B)** The 2D model of the molecular docking of the ertugliflozin-Keap1 complex. **(C)** The 3D model of the molecular docking of the ertugliflozin-Keap1 complex. **(D)** Immunostaining image of Nrf2 in renal tubules of the sham group. **(E)** Immunostaining image of Nrf2 in renal tubules of the I/R group. **(F)** Immunostaining image of Nrf2 in renal tubules of the I/R+Veh group. **(G)** Immunostaining image of Nrf2 in renal tubules of the I/R+EGZ group. The sham group underwent laparotomy without induction of the I/R model. The I/R, I/R+Veh, and I/R+EGZ groups were subjected to 30 minutes of bilateral renal ischemia and 24 hours of reperfusion. The I/R+Veh and I/R+EGZ groups received the solvent or 20 mg/kg of ertugliflozin intraperitoneally one hour before ischemia induction, respectively. Molecular docking was performed using the MOE software 2015. Nrf2 was measured in renal tissue by IHC staining. Data expressed as Mean ± SD, S=-6.05703, RMSD=0.731347, $^{**}p < 0.01$, $^{***}p < 0.001$, $^{****}p < 0.0001$.

Table 2. Statistical analysis of cytoplasmic and nuclear Nrf2 among the study groups.

-	Tukey's Multiple Comparisons	Mean Difference	*p*-value
Cytoplasmic Nrf2	Sham *vs.* I/R	-4.833	0.9560
	Sham *vs.* I/R+Veh	-3.333	0.9847
	Sham *vs.* I/R+EGZ	-3.333	0.9847
	I/R *vs.* I/R+Veh	1.500	0.9985
	I/R *vs.* I/R+EGZ	1.500	0.9985
	I/R+Veh *vs.* I/R+EGZ	0.000	>0.9999
-	**Mann–Whitney U test**	**Mean Difference**	***p*-value**
Nuclear Nrf2	Sham *vs.* I/R	0.00	1.000
	Sham *vs.* I/R+Veh	0.00	1.000
	Sham *vs.* I/R+EGZ	-12.00	0.002
	I/R *vs.* I/R+Veh	0.00	1.000
	I/R *vs.* I/R+EGZ	-12.00	0.002
	I/R+Veh *vs.* I/R+EGZ	-12.00	0.002

Note: I/R Ischemia/Reperfusion, Veh vehicle, EGZ ertugliflozin, Nrf2 Nuclear Factor Erythroid 2-related factor 2.

Table 3. Statistical analysis of MLKL and histopathological examination among the study groups.

-	Tukey's Multiple Comparisons	Mean Difference	*p*-value
MLKL	Sham *vs.* I/R	-141.7	<0.0001
	Sham *vs.* I/R+Veh	-125.2	<0.0001
	Sham *vs.* I/R+EGZ	-20.33	0.7919
	I/R *vs.* I/R+Veh	16.50	0.8753
	I/R *vs.* I/R+EGZ	121.3	0.0001
	I/R+Veh *vs.* I/R+EGZ	104.8	0.0006
-	**Mann–Whitney U test**	**Mean Difference**	***p*-value**
Histopathological Examination	Sham *vs.* I/R	-3.833	0.002
	Sham *vs.* I/R+Veh	-4.000	0.002
	Sham *vs.* I/R+EGZ	-2.833	0.002
	I/R *vs.* I/R+Veh	-0.167	0.699
	I/R *vs.* I/R+EGZ	1.000	0.009
	I/R+Veh *vs.* I/R+EGZ	1.167	0.002

Note: I/R Ischemia/Reperfusion, Veh Vehicle, EGZ ertugliflozin, MLKL Mixed Lineage Kinase Domain-Like Protein.

3.4. Ertugliflozin Reduces Inflammation in the Renal IRI Model

For assessing the impact of ertugliflozin on inflammation, TNF-α, IL-1β, and NF-κB levels were measured in renal tissue. TNF-α, IL-1β, and NF-κB levels in the I/R and vehicle groups were substantially elevated compared with the sham group ($p < 0.05$). Ertugliflozin exhibited a remarkable reduction relative to the I/R group for TNF-α ($p < 0.01$), IL-1β ($p < 0.05$), and NF-κB ($p < 0.01$). Furthermore, a significant reduction was also observed in contrast with the I/R + Veh group for NF-κB and TNF-α ($p < 0.05$). A non-noticeable difference between I/R and I/R + Veh groups was found in all measured inflammatory markers ($p > 0.05$) (Fig. **1**).

3.5. Ertugliflozin Downregulates the Markers of the Necroptosis Pathway in the Renal IRI Model

The extent of gene expression of RIPK1 was measured in renal tissue. The induction of the I/R model dramatically elevated the gene expression level of RIPK1 in the I/R and vehicle groups as opposed to the sham group ($p < 0.0001$). In contrast, ertugliflozin substantially decreased the level of RIPK1 in the I/R + EGZ group, compared to that of I/R and I/R + Veh groups ($p < 0.0001$). Instead, RIPK1 exhibited no substantial variation between I/R and I/R + Veh groups ($p > 0.05$) (Fig. **3**). Regarding the role of ertugliflozin on MLKL, MLKL was measured in renal tissue. The induction of renal IRI remarkably escalated MLKL in I/R and I/R + Veh groups as opposed to the sham group ($p < 0.01$). Conversely, the ertugliflozin-treated group demonstrated a considerable reduction in MLKL, unlike the IRI-induced and vehicle groups ($p < 0.05$) (Table **3** and Fig. **3**).

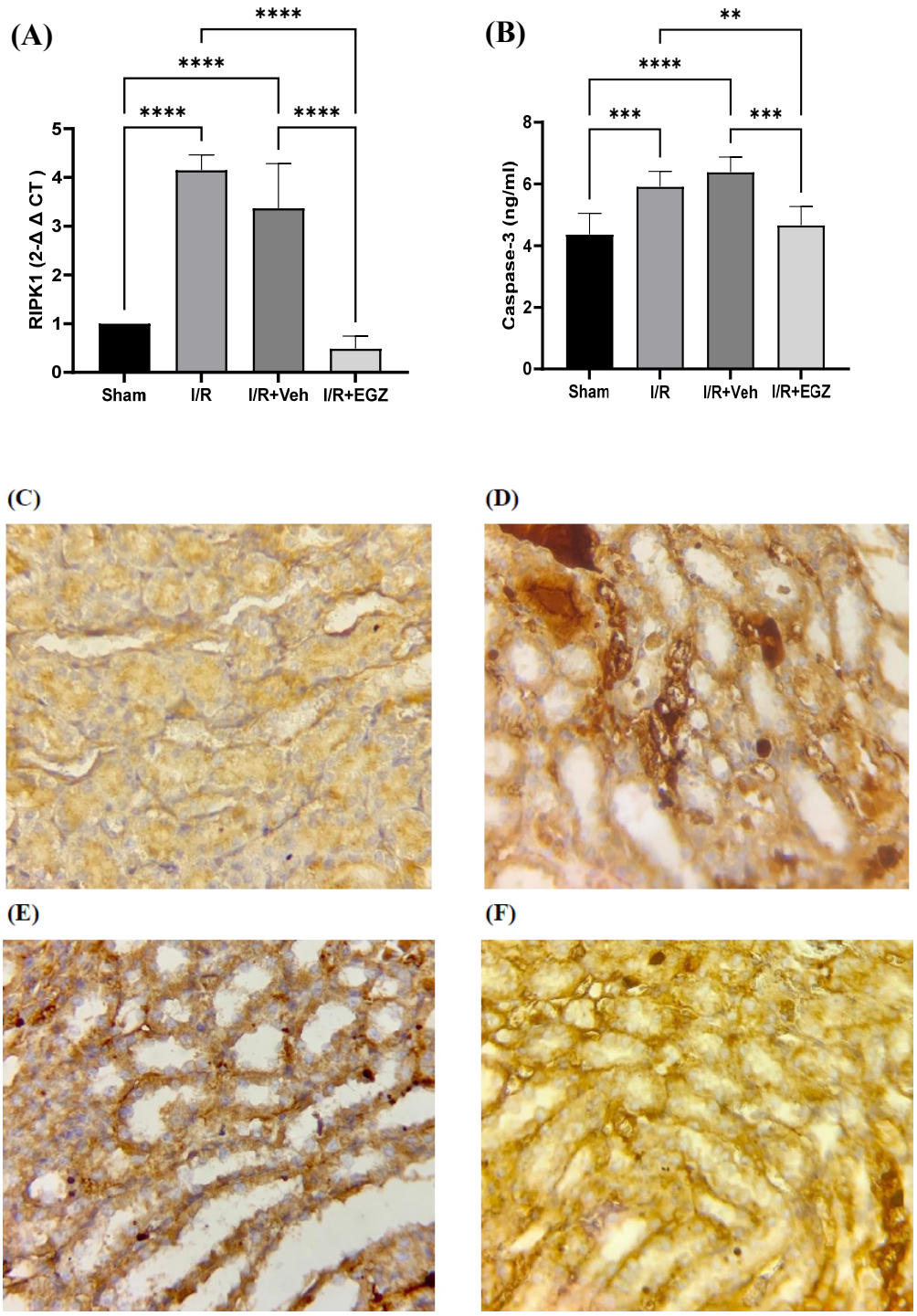

Fig. (3). Effects of ertugliflozin on the necroptosis pathway, (**A**) RIPK1 (Fold change), **(B)** Caspase-3, **(C)** Immunostaining image of MLKL in renal tubules of the sham group, **(D)** Immunostaining image of MLKL in renal tubules of the I/R group, **(E)** Immunostaining image of MLKL in renal tubules of the I/R+Veh group, **(F)** Immunostaining image of MLKL in renal tubules of the I/R+EGZ groups. The sham group underwent laparotomy without induction of the I/R model. The I/R, I/R+Veh, and I/R+EGZ groups were subjected to 30 minutes of bilateral renal ischemia and 24 hours of reperfusion. The I/R+Veh and I/R+EGZ groups received the solvent or 20 mg/kg of ertugliflozin intraperitoneally one hour before ischemia induction, respectively. RIPK1 was measured in renal tissue by RT-qPCR; the fold change was calculated by the 2-ΔΔCT method. Caspase-3 was measured in renal tissue using the ELISA technique. MLKL was measured in renal tissue by IHC staining. Data expressed as Mean ± SD, $^{**}p < 0.01$, $^{***}p < 0.001$, $^{****}p < 0.0001$.

3.6. Ertugliflozin Mitigates Apoptosis in the Renal IRI Model

The caspase-3 level exhibited a substantial increment in I/R and I/R + Veh groups relative to the sham group ($p < 0.001$ *vs*. I/R, $p < 0.0001$ *vs*. I/R + Veh). Conversely, ertugliflozin in I/R + EGZ remarkably reduced the caspase-3 level relative to the I/R group ($p < 0.01$) and I/R + Veh group ($p < 0.001$). However, the I/R group did not exhibit remarkable differences from the vehicle group ($p > 0.05$) (Fig. **3**).

3.7. Ertugliflozin Enhanced the Histopathological Findings in the Renal IRI Model

Renal tubular histology was normal in the sham group (Fig. **4A**). The histopathological findings in I/R include cellular swelling, inflammation, edema, cytoplasmic eosinophilia, and loss of brush border ($p < 0.0001$) (Fig. **4B**). The vehicle group had morphological features like those of the I/R group ($p > 0.05$) (Fig. **4C**). As in Fig. (**4D**), there was a substantial reduction of microscopic findings in the group treated with ertugliflozin as opposed to the I/R and I/R+Veh groups ($p < 0.05$) (Table **3** and Fig. **4**).

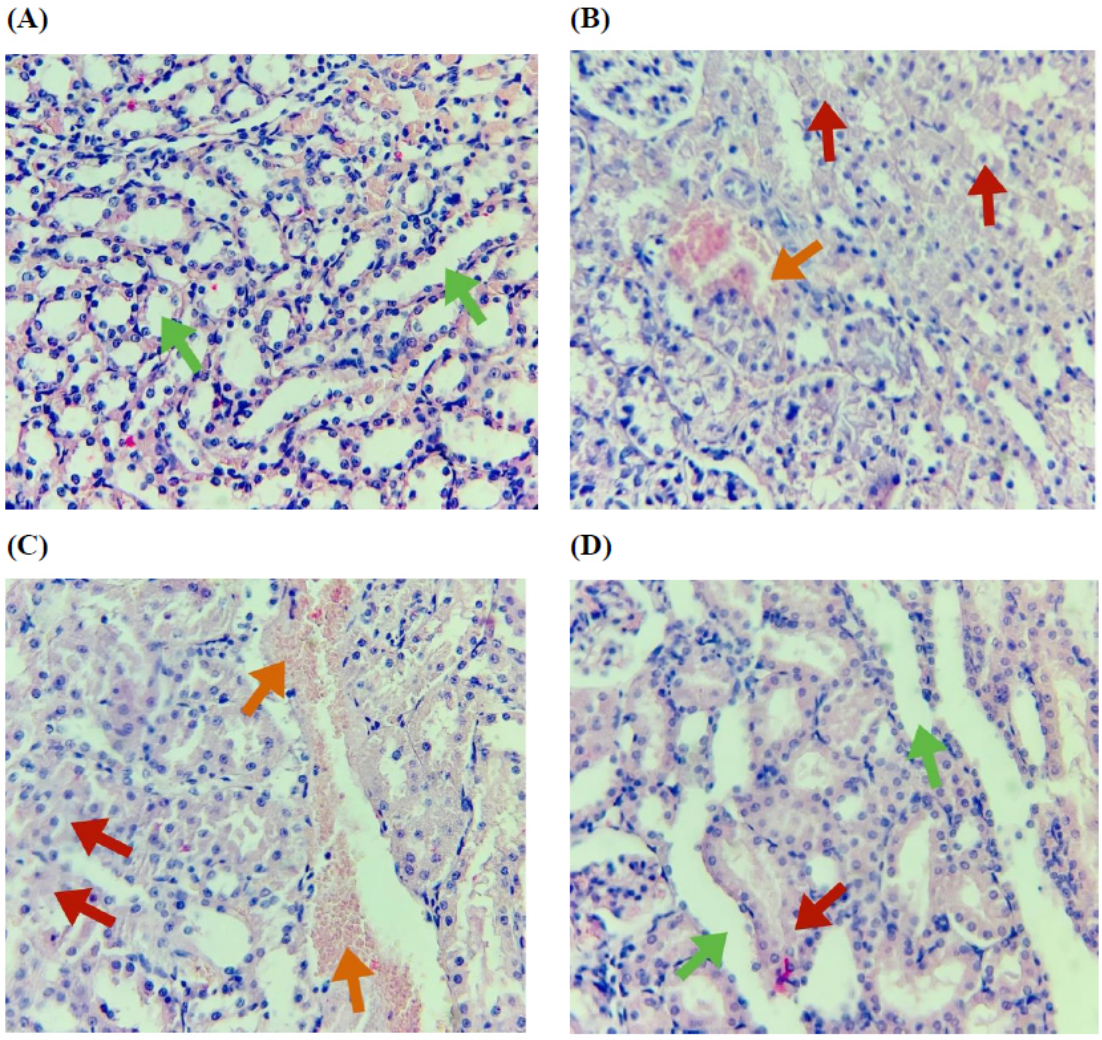

Fig. (4). Histopathological photomicrographs of the study groups. **(A)** Sham group: Normal histology, **(B)** I/R group: Renal tubules showing a damage score of 4, affecting 80% of the observed tubules, **(C)** I/R+Veh group: Renal tubules showing a damage score of 4, affecting 85% of the observed tubules, **(D)** I/R+EGZ group: Renal tubules showing a damage score of 2, affecting 40% of the observed tubules. The sham group underwent laparotomy without induction of the I/R model. The I/R, I/R+Veh, and I/R+EGZ groups were subjected to 30 minutes of bilateral renal ischemia and 24 hours of reperfusion. The I/R+Veh and I/R+EGZ groups received the solvent or 20 mg/kg of ertugliflozin intraperitoneally one hour before ischemia induction, respectively. **Green arrow** (normal renal tubules), **red arrow** (disruption of renal tubular integrity), **orange arrow** (vascular congestion and hemorrhage). Histopathological examination was done by H&E staining. Magnification X400. Data expressed as Mean ± SD.

4. DISCUSSION

AKI is an abrupt deficiency of renal function, resulting in an elevation in serum creatinine and/or a reduction in urine production, which is associated with elevated mortality, morbidity, hospitalization, and chronic kidney disease [32]. Renal IRI is a sequence of complex events that involve a reduction in blood supply followed by a recovery of perfusion and oxygenation to the kidneys [1]. It is a life-threatening leading cause of AKI. It is a multifaceted process encompassing various mechanisms and molecular pathways of cellular dysfunction and death, including necroptosis and apoptosis [33]. It is worth noting that there are no approved pharmacotherapeutic agents to prevent, treat, or improve AKI recovery [34, 35]. The development of novel biomarkers for AKI is critically required for early diagnosis, severity assessment, and monitoring of tubular damage. Using serum creatinine and blood urea as biomarkers in renal diseases lacks sensitivity and specificity. Furthermore, these biomarkers assess the functional but not the damaging changes [36, 37]. The current study showed that induction of the I/R model significantly elevated the KIM-1 level. In contrast, administering 20 mg/kg of ertugliflozin one hour before ischemia induction substantially lowered KIM-1 concentration. These findings align with those of Liu *et al*. [38], who reported that taking ertugliflozin reduced KIM-1 levels in participants. KIM-1 is overexpressed in proximal epithelial cells in response to stressful conditions like IRI and toxicity, transforming epithelial cells into phagocytic cells, alleviating and repairing the tubular damage, inducing cellular autophagy, and disposing of necrotic tissue and apoptotic cells [39, 40]. Nrf2 is a master orchestrator that regulates the genetic expression of antioxidant and phase II enzymes and is physiologically inhibited by Keap1 [41]. Several chemicals and ROS dissociate Keap1 from Nrf2 in the cytoplasm, leading to Nrf2 activation, nuclear translocation, and upregulation of various cytoprotective genes [42]. The present study measured both cytoplasmic and nuclear Nrf2. Cytoplasmic Nrf2 levels did not increase in the ertugliflozin-treated group; however, a substantial elevation in nuclear Nrf2 levels was observed with the ertugliflozin pretreatment. To point out the mechanism by which ertugliflozin exerts its effect, we docked ertugliflozin with Keap1. The *in-silico* study results showed that ertugliflozin interacts with Keap1 through His129 and His154 near the critical Cys151. Further studies are needed to highlight the significance of this binding. The overall findings showed that ertugliflozin increased the nuclear translocation of Nrf2, possibly by affecting the Nrf2-Keap1 complex. NF-κB is a transcriptional factor that regulates several cellular processes, including inflammation, tissue injury, and repair [43]. The reperfusion phase of renal IRI can induce ROS and NF-κB expression, with the subsequent increase in TNF-α and IL-1β [44]. Inversely, activation of Nrf2 can inhibit the NFκB pathway by upregulating antioxidant genes, thus decreasing pro-inflammatory cytokines [45]. Hence, we evaluated the NF-κB, TNF-α, and IL-1β levels in renal tissue. The current study showed that these biomarkers are elevated in rats following I/R induction. At the same time, ertugliflozin reduced these biomarkers in contrast to the I/R group. Abd Uljaleel and Hassan [20] reported that ertugliflozin markedly reduced TNF-α and IL-1β in the acute lung injury in mice. The interaction of TNF-α with its receptor, TNFR1, initiates multiple pathways with distinct outcomes, including cellular survival, apoptosis, and necroptosis. Necroptosis is thought to significantly contribute to the development of renal IRI [46]. Necrosome is the core complex of necroptosis, comprising RIPK1, RIPK3, and MLKL [47]. After phosphorylation and activation of RIPK1 and RIPK3, the RIPK1-RIPK3 complex is recruited, and MLKL is phosphorylated, triggering MLKL oligomerization. Afterward, this cluster of phosphorylated MLKL travels to the plasma membrane to trigger necroptosis by forming a group of pores that damage the membrane or by regulating the influx of ion channels [48]. To assess the effects of ertugliflozin on cell survival and death in the AKI model, we first studied the molecular pathway of necroptosis by measuring the gene expression of RIPK1 by RT-qPCR and MLKL levels by IHC. The results showed that induction of the I/R model dramatically increased the levels of both RIPK1 and MLKL. Simultaneously, ertugliflozin remarkably lowered the levels of these markers in contrast to the I/R and vehicle groups. Then, we measured caspase-3 in renal tissue as a marker of apoptosis. Caspase-3 is an executioner caspase and a key apoptosis regulator [49]. The present study showed that ertugliflozin administration markedly reduced caspase-3 levels, which were greatly elevated in the I/R and vehicle groups. Consistent with our results, the research of Moellmann *et al*. [50] showed that ertugliflozin decreased apoptosis by lowering the caspase-3 levels in the mice cardiac tissue. The histopathological examination further emphasizes the nephroprotective effect of ertugliflozin on renal parenchyma, showing that the treated group had improved histological findings. These results align with Abd Uljaleel and Hassan [20] in mice's lungs. Our results strongly imply that ertugliflozin effectively reduces oxidation, inflammation, necroptosis, apoptosis, and necrosis.

5. LIMITATIONS OF THE STUDY

This study had a few limitations. The study used only male rats; future research on both sexes is needed to investigate hormonal effects. Furthermore, we administered ertugliflozin before ischemia induction; further studies can administer it before and after ischemia induction to evaluate the preventive and therapeutic effects of ertugliflozin.

CONCLUSION

The current study demonstrated that the induction of IRI in rats' kidneys substantially increased inflammation and cell death. Conversely, ertugliflozin showed marked nephroprotective effects evidenced by reduced inflammation, necroptosis, apoptosis, and necrosis through activation of Nrf2 and inhibition of RIPK1/MLKL pathways.

AUTHORS' CONTRIBUTIONS

The authors confirm their contribution to the paper as follows: A.F.J.: Draft manuscript; A.M.J.: Methodology. All authors reviewed the results and approved the final version of the manuscript.

LIST OF ABBREVIATIONS

IRI	=	Ischemia/Reperfusion Injury
ATP	=	Adenosine Triphosphate
ROS	=	Reactive Oxygen Species
IHC	=	Immunohistochemistry
H&E	=	Hematoxylin and Eosin
PBS	=	Phosphate Buffer Saline

ETHICS APPROVAL AND CONSENT TO PARTICIPATE

The Central Committee of Bioethics at the University of Kufa, Iraq, approved all the procedures and experimental design (Approval No. 20554) on August 29, 2024.

HUMAN AND ANIMAL RIGHTS

This study adheres to internationally accepted standards for animal research, following the 3Rs principle. The ARRIVE guidelines were employed for reporting experiments involving live animals, promoting ethical research practices.

The policy of the University of Kufa for scientific purposes is followed in the care and usage of animals.

CONSENT FOR PUBLICATION

Not applicable.

AVAILABILITY OF DATA AND MATERIALS

The data supporting the findings of the article will be available from the corresponding author [A.F.J] upon reasonable request.

FUNDING

None.

CONFLICT OF INTEREST

The authors declare no conflict of interest, financial or otherwise.

ACKNOWLEDGEMENTS

Declared none.

REFERENCES

[1] Karimi, F.; Maleki, M.; Nematbakhsh, M. View of the renin-angiotensin system in acute kidney injury induced by renal ischemia-reperfusion injury. *J. Renin Angiotensin Aldosterone Syst.,* **2022**, *2022*, 9800838. http://dx.doi.org/10.1155/2022/9800838 PMID: 36320442

[2] Soares, R.O.S.; Losada, D.M.; Jordani, M.C.; Évora, P.; Castro-e-Silva, O. Ischemia/reperfusion injury revisited: An overview of the latest pharmacological strategies. *Int. J. Mol. Sci.,* **2019**, *20*(20), 5034. http://dx.doi.org/10.3390/ijms20205034 PMID: 31614478

[3] Luo, J.; Pei, J.; Yu, C.; Tian, X.; Zhang, J.; Shen, L.; Hua, Y.; Wei, G.H. Exploring the role of Hmox1 in ferroptosis and immune infiltration during renal ischemia-reperfusion injury. *Ren. Fail.,* **2023**, *45*(2), 2257801. http://dx.doi.org/10.1080/0886022X.2023.2257801 PMID: 38532724

[4] Bonventre, J.V.; Yang, L. Cellular pathophysiology of ischemic acute kidney injury. *J. Clin. Invest.,* **2011**, *121*(11), 4210-4221. http://dx.doi.org/10.1172/JCI45161 PMID: 22045571

[5] Aksu, U.; Ergin, B.; Bezemer, R.; Kandil, A.; Milstein, D.M.J.; Demirci-Tansel, C.; Ince, C. Scavenging reactive oxygen species using tempol in the acute phase of renal ischemia/reperfusion and its effects on kidney oxygenation and nitric oxide levels. *Intensive Care Med. Exp.,* **2015**, *3*(1), 21. http://dx.doi.org/10.1186/s40635-015-0057-y PMID: 26215821

[6] Pei, J.; Tian, X.; Yu, C.; Luo, J.; Zhang, J.; Hua, Y.; Wei, G. GPX3 and GSTT1 as biomarkers related to oxidative stress during renal ischemia reperfusion injuries and their relationship with immune infiltration. *Front. Immunol.,* **2023**, *14*, 1136146. http://dx.doi.org/10.3389/fimmu.2023.1136146 PMID: 37033969

[7] Lin, L.; Wu, Q.; Lu, F.; Lei, J.; Zhou, Y.; Liu, Y.; Zhu, N.; Yu, Y.; Ning, Z.; She, T.; Hu, M. Nrf2 signaling pathway: Current status and potential therapeutic targetable role in human cancers. *Front. Oncol.,* **2023**, *13*, 1184079. http://dx.doi.org/10.3389/fonc.2023.1184079 PMID: 37810967

[8] Ulasov, A.V.; Rosenkranz, A.A.; Georgiev, G.P.; Sobolev, A.S. Nrf2/Keap1/ARE signaling: Towards specific regulation. *Life Sci.,* **2022**, *291*, 120111. http://dx.doi.org/10.1016/j.lfs.2021.120111 PMID: 34732330

[9] Wei, W.; Ma, N.; Fan, X.; Yu, Q.; Ci, X. The role of Nrf2 in acute kidney injury: Novel molecular mechanisms and therapeutic approaches. *Free Radic. Biol. Med.,* **2020**, *158*, 1-12. http://dx.doi.org/10.1016/j.freeradbiomed.2020.06.025 PMID: 32663513

[10] Ma, D.; Wang, X.; Liu, J.; Cui, Y.; Luo, S.; Wang, F. The development of necroptosis: What we can learn. *Cell Stress Chaperones,* **2023**, *28*(6), 969-987. http://dx.doi.org/10.1007/s12192-023-01390-5 PMID: 37995025

[11] Meng, Y.; Sandow, J.J.; Czabotar, P.E.; Murphy, J.M. The regulation of necroptosis by post-translational modifications. *Cell Death Differ.,* **2021**, *28*(3), 861-883. http://dx.doi.org/10.1038/s41418-020-00722-7 PMID: 33462412

[12] Ye, K.; Chen, Z.; Xu, Y. The double-edged functions of necroptosis. *Cell Death Dis.,* **2023**, *14*(2), 163. http://dx.doi.org/10.1038/s41419-023-05691-6 PMID: 36849530

[13] Hu, X.; Wang, Z.; Kong, C.; Wang, Y.; Zhu, W.; Wang, W.; Li, Y.; Wang, W.; Lu, S. Necroptosis: A new target for prevention of osteoporosis. *Front. Endocrinol.,* **2022**, *13*, 1032614. http://dx.doi.org/10.3389/fendo.2022.1032614 PMID: 36339402

[14] Nguyen, V.K.; White, J.R., Jr Overview of ertugliflozin. *Clin. Diabetes,* **2019**, *37*(2), 176-178. http://dx.doi.org/10.2337/cd18-0097 PMID: 31057225

[15] Heymsfield, S.B.; Raji, A.; Gallo, S.; Liu, J.; Pong, A.; Hannachi, H.; Terra, S.G. Efficacy and safety of ertugliflozin in patients with overweight and obesity with type 2 diabetes mellitus. *Obesity,* **2020**, *28*(4), 724-732. http://dx.doi.org/10.1002/oby.22748 PMID: 32202075

[16] Vallon, V.; Verma, S. Effects of SGLT2 inhibitors on kidney and cardiovascular function. *Annu. Rev. Physiol.,* **2021**, *83*(1), 503-528. http://dx.doi.org/10.1146/annurev-physiol-031620-095920 PMID: 33197224

[17] Sahasrabudhe, V.; Matschke, K.; Shi, H.; Hickman, A.; Kong, A.; Spong, B.R.; Nickerson, B.; Arora, K.K. Relative bioavailability of ertugliflozin tablets containing the amorphous form *versus* tablets containing the cocrystal form. *Int. J. Clin. Pharmacol. Ther.,* **2022**, *60*(7), 317-326. http://dx.doi.org/10.5414/CP204212 PMID: 35575420

[18] Fediuk, D.J.; Nucci, G.; Dawra, V.K.; Cutler, D.L.; Amin, N.B.; Terra, S.G.; Boyd, R.A.; Krishna, R.; Sahasrabudhe, V. Overview of the clinical pharmacology of ertugliflozin, a novel sodium-glucose cotransporter 2 (SGLT2) inhibitor. *Clin. Pharmacokinet.,* **2020**, *59*(8), 949-965. http://dx.doi.org/10.1007/s40262-020-00875-1 PMID: 32337660

[19] Arifin, W.N.; Zahiruddin, W.M. Sample size calculation in animal studies using resource equation approach. *Malays. J. Med. Sci.,* **2017**, *24*(5), 101-105. http://dx.doi.org/10.21315/mjms2017.24.5.11 PMID: 29386977

[20] Abd Uljaleel, A.Q.; Hassan, E.S. Protective effect of ertugliflozin against acute lung injury caused by endotoxemia model in mice. *Iran. J. War Public Health.,* **2023**, *15*, 67-75. http://dx.doi.org/10.58209/ijwph.15.1.67

[21] Basalay, M.; Arjun, S.; Davidson, S.; Yellon, D. The role of parasympathetic mechanisms in the infarct-limiting effect of SGLT2 inhibitor Ertugliflozin. *Biorxiv,* **2021**, 2021.10. http://dx.doi.org/10.1101/2021.10.01.462765

[22] Jallawee, H.Q.; Janabi, A.M. Trandolapril improves renal ischemia-reperfusion injury in adult male rats *via* activation of the autophagy pathway and inhibition of inflammation, oxidative stress, and apoptosis. *J. Biosci. Appl. Res.,* **2024**, *10*(6), 114-127. http://dx.doi.org/10.21608/jbaar.2024.315239.1077

[23] Kobroob, A.; Kongkaew, A.; Wongmekiat, O. Melatonin reduces aggravation of renal ischemia–reperfusion injury in obese rats by maintaining mitochondrial homeostasis and integrity through AMPK/PGC-1α/SIRT3/SOD2 activation. *Curr. Issues Mol. Biol.,* **2023**, *45*(10), 8239-8254. http://dx.doi.org/10.3390/cimb45100520 PMID: 37886963

[24] Alkhafaji, G.A.; Janabi, A.M. Protective effects of bexagliflozin on renal function in a rat model of ischemia-reperfusion injury; an experimental animal study. *J. Nephropharmacol.,* **2025**, *14*, e12760. http://dx.doi.org/10.34172/npj.2025.12760

[25] Alsaaty, E.H.; Janabi, A.M. Moexipril improves renal ischemia/reperfusion injury in adult male rats. *J. Contemp. Med. Sci.,* **2024**, *10*(1), 25-30. http://dx.doi.org/10.22317/jcms.v10i1.1477

[26] Alaasam, E.R.; Janabi, A.M.; Al-Buthabhak, K.M.; Almudhafar, R.H.; Hadi, N.R.; Alexiou, A.; Papadakis, M.; Abo-El Fetoh, M.E.; Fouad, D.; El-Saber Batiha, G. Nephroprotective role of resveratrol in renal ischemia-reperfusion injury: A preclinical study in Sprague-Dawley rats. *BMC Pharmacol. Toxicol.,* **2024**, *25*(1), 82. http://dx.doi.org/10.1186/s40360-024-00809-8 PMID: 39468702

[27] Alaasam, E.R.; Janabi, A.M. Erythropoietin protects against renal ischemia/reperfusion injury in rats *via* inhibition of oxidative stress, inflammation and apoptosis. *J. Contemp. Med. Sci.,* **2023**, *9*(4), 233-238. http://dx.doi.org/10.22317/jcms.v9i4.1405

[28] Alkhafaji, G.A.; Janabi, A.M. GIP/GLP-1 dual agonist tirzepatide ameliorates renal ischemia/reperfusion damage in rats. *Int. J. Appl. Pharm.,* **2025**, *17*(2), 165-173. http://dx.doi.org/10.22159/ijap.2025v17i2.53156

[29] Hassoon, M.F.; Hadi, N.R.; Mahboba, W.; Jawad, D.; Hussien, Y.A.; Abdulkhaleq, M.A. Nephroprotective potential effect of canagliflozin in renal ischemia reperfusion injury in rat model: role of Nrf2 pathway. *SRP.,* **2019**, *10*(2), 60-69. http://dx.doi.org/10.5530/srp.2019.2.11

[30] Charafe-Jauffret, E.; Tarpin, C.; Bardou, V.J.; Bertucci, F.; Ginestier, C.; Braud, A.C.; Puig, B.; Geneix, J.; Hassoun, J.; Birnbaum, D.; Jacquemier, J.; Viens, P. Immunophenotypic analysis of inflammatory breast cancers: Identification of an 'inflammatory signature'. *J. Pathol.,* **2004**, *202*(3), 265-273. http://dx.doi.org/10.1002/path.1515 PMID: 14991891

[31] Parris, T.Z.; Aziz, L.; Kovács, A.; Hajizadeh, S.; Nemes, S.; Semaan, M.; Chen, C.Y.; Karlsson, P.; Helou, K. Clinical relevance of breast cancer-related genes as potential biomarkers for oral squamous cell carcinoma. *BMC Cancer,* **2014**, *14*(1), 324. http://dx.doi.org/10.1186/1471-2407-14-324 PMID: 24885002

[32] Connell, A.; Laing, C. Acute kidney injury. *Clin. Med.,* **2015**, *15*(6), 581-584. http://dx.doi.org/10.7861/clinmedicine.15-6-581 PMID: 26621953

[33] Li, C.; Yu, Y.; Zhu, S.; Hu, Y.; Ling, X.; Xu, L.; Zhang, H.; Guo, K. The emerging role of regulated cell death in ischemia and reperfusion-induced acute kidney injury: Current evidence and future perspectives. *Cell Death Discov.,* **2024**, *10*(1), 216. http://dx.doi.org/10.1038/s41420-024-01979-4 PMID: 38704372

[34] Doi, K. Identifying the right target for new drugs in acute kidney injury: A long way off? *Kidney Int. Rep.,* **2023**, *8*(7), 1287-1289. http://dx.doi.org/10.1016/j.ekir.2023.05.025 PMID: 37441491

[35] Pickkers, P.; Murray, P.T.; Ostermann, M. New drugs for acute kidney injury. *Intensive Care Med.,* **2022**, *48*(12), 1796-1798. http://dx.doi.org/10.1007/s00134-022-06859-y PMID: 35999470

[36] Bonventre, J.V. Kidney injury molecule-1 (KIM-1): A urinary biomarker and much more. *Nephrol. Dial. Transplant.,* **2009**, *24*(11), 3265-3268. http://dx.doi.org/10.1093/ndt/gfp010 PMID: 19318357

[37] Oh, D.J. A long journey for acute kidney injury biomarkers. *Ren. Fail.,* **2020**, *42*(1), 154-165. http://dx.doi.org/10.1080/0886022X.2020.1721300 PMID: 32050834

[38] Liu, H.; Sridhar, V.S.; Lovblom, L.E.; Lytvyn, Y.; Burger, D.; Burns, K.; Brinc, D.; Lawler, P.R.; Cherney, D.Z.I. Markers of kidney injury, inflammation, and fibrosis associated with ertugliflozin in patients with CKD and diabetes. *Kidney Int. Rep.,* **2021**, *6*(8), 2095-2104. http://dx.doi.org/10.1016/j.ekir.2021.05.022 PMID: 34386658

[39] Song, J.; Yu, J.; Prayogo, G.W.; Cao, W.; Wu, Y.; Jia, Z.; Zhang, A. Understanding kidney injury molecule 1: A novel immune factor in kidney pathophysiology. *Am. J. Transl. Res.,* **2019**, *11*(3), 1219-1229. PMID: 30972157

[40] Tanase, D.M.; Gosav, E.M.; Radu, S.; Costea, C.F.; Ciocoiu, M.; Carauleanu, A.; Lacatusu, C.M.; Maranduca, M.A.; Floria, M.; Rezus, C. The predictive role of the biomarker kidney molecule-1 (KIM-1) in acute kidney injury (AKI) cisplatin-induced nephrotoxicity. *Int. J. Mol. Sci.,* **2019**, *20*(20), 5238. http://dx.doi.org/10.3390/ijms20205238 PMID: 31652595

[41] Ngo, V.; Duennwald, M.L. Nrf2 and oxidative stress: A general overview of mechanisms and implications in human disease. *Antioxidants,* **2022**, *11*(12), 2345. http://dx.doi.org/10.3390/antiox11122345 PMID: 36552553

[42] He, F.; Ru, X.; Wen, T. NRF2, a transcription factor for stress response and beyond. *Int. J. Mol. Sci.,* **2020**, *21*(13), 4777. http://dx.doi.org/10.3390/ijms21134777 PMID: 32640524

[43] Ghazi, A; Abood, SH; Alaqouli, H; Hadi, NR; Majeed, SA; Janabi, AM Ibudilast and octreotide can ameliorate acute pancreatitis *via* down-regulation of the inflammatory cytokines and Nuclear Factor- Kappa B expression. *Ann. Trop. Med. Public Health.,* **2019**, *22*(4), 1-7. http://dx.doi.org/10.36295/ASRO.2019.22041

[44] Khajuria, A.; Tay, C.; Shi, J.; Zhao, H.; Ma, D. Anesthetics attenuate ischemia–reperfusion induced renal injury: Effects and mechanisms. *Acta Anaesthesiol. Taiwan.,* **2014**, *52*(4), 176-184. http://dx.doi.org/10.1016/j.aat.2014.10.001 PMID: 25477261

[45] Chang, K.H.; Chen, C.M. The role of NRF2 in trinucleotide repeat expansion disorders. *Antioxidants,* **2024**, *13*(6), 649. http://dx.doi.org/10.3390/antiox13060649 PMID: 38929088

[46] Pefanis, A.; Bongoni, A.K.; McRae, J.L.; Salvaris, E.J.; Fisicaro, N.; Murphy, J.M.; Ierino, F.L.; Cowan, P.J. Dynamics of necroptosis in kidney ischemia-reperfusion injury. *Front. Immunol.,* **2023**, *14*, 1251452. http://dx.doi.org/10.3389/fimmu.2023.1251452 PMID: 38022500

[47] Dai, W.; Cheng, J.; Leng, X.; Hu, X.; Ao, Y. The potential role of necroptosis in clinical diseases (Review). *Int. J. Mol. Med.,* **2021**, *47*(5), 89. http://dx.doi.org/10.3892/ijmm.2021.4922 PMID: 33786617

[48] Seo, J.; Nam, Y.W.; Kim, S.; Oh, D.B.; Song, J. Necroptosis molecular mechanisms: Recent findings regarding novel necroptosis regulators. *Exp. Mol. Med.,* **2021**, *53*(6), 1007-1017. http://dx.doi.org/10.1038/s12276-021-00634-7 PMID: 34075202

[49] Yadav, P.; Yadav, R.; Jain, S.; Vaidya, A. Caspase-3: A primary target for natural and synthetic compounds for cancer therapy. *Chem. Biol. Drug Des.*, **2021**, *98*(1), 144-165. http://dx.doi.org/10.1111/cbdd.13860 PMID: 33963665

[50] Moellmann, J.; Mann, P.A.; Kappel, B.A.; Kahles, F.; Klinkhammer, B.M.; Boor, P.; Kramann, R.; Ghesquiere, B.; Lebherz, C.; Marx, N.; Lehrke, M. The sodium-glucose co-transporter-2 inhibitor ertugliflozin modifies the signature of cardiac substrate metabolism and reduces cardiac MTOR signalling, endoplasmic reticulum stress and apoptosis. *Diabetes Obes. Metab.,* **2022**, *24*(11), 2263-2272. http://dx.doi.org/10.1111/dom.14814 PMID: 35801343